ISSN 1674-1056
http://cpb.iphy.ac.cn
http://iopscience.iop.org/cpb
中国物理 B
Chinese Physics
中国物理
Chinese Physics B

Optical power limiting of ultrashort hyper-Gaussian pulses in cascade three-level system

Ji-Cai Liu(刘纪彩), Fen-Fen Guo(郭芬芬), Ya-Nan Zhao(赵亚男), Xing-Zhe Li(李兴哲)

Citation: Chin. Phys. B . 2018, 27(10): 104209. **doi:** 10.1088/1674-1056/27/10/104209

Journal homepage: http://cpb.iphy.ac.cn; http://iopscience.iop.org/cpb

What follows is a list of articles you may be interested in

Etching-assisted femtosecond laser microfabrication

Monan Liu(刘墨南), Mu-Tian Li(李木天), Han Yang(杨罕), Hong-Bo Sun(孙洪波)
Chin. Phys. B . 2018, 27(9): 094212. **doi:** 10.1088/1674-1056/27/9/094212

Enhancement and modulation of terahertz radiation by multi-color laser pulses

Min-Jie Pei(裴敏洁), Chen-Hui Lu(卢晨晖), Xian-Wei Wang(王宪位), Zhen-Rong Sun(孙真荣), Shi-An Zhang(张诗按)
Chin. Phys. B . 2018, 27(8): 084209. **doi:** 10.1088/1674-1056/27/8/084209

High-power ultraviolet 278-nm laser from fourth-harmonic generation of an Nd: YAG amplifier in CsB_3O_5 crystal

Miao He(何苗), Feng Yang(杨峰), Cheng Dong(董程), Zhi-Chao Wang(王志超), Lei Yuan(袁磊), Yi-Ting Xu(徐一汀), Guo-Chun Zhang(张国春), Zhi-Min Wang(王志敏), Yong Bo(薄勇), Qin-Jun Peng(彭钦军), Da-Fu Cui(崔大复), Yi-Cheng Wu(吴以成), Zu-Yan Xu(许祖彦)
Chin. Phys. B . 2018, 27(5): 054211. **doi:** 10.1088/1674-1056/27/5/054211

Effect of multiple rescattering processes on harmonic emission in spatially inhomogeneous field

Cai-Ping Zhang(张彩萍), Chang-Long Xia(夏昌龙), Xiang-Fu Jia(贾祥富), Xiang-Yang Miao(苗向阳)
Chin. Phys. B . 2018, 27(3): 034206. **doi:** 10.1088/1674-1056/27/3/034206

Two-color laser wavelength effect on intense terahertz generation in air

Shufen Li(李淑芬), Chenhui Lu(卢晨晖), Chengshuai Yang(杨承帅), Yanzhong Yu(余燕忠), Zhenrong Sun(孙真荣), Shian Zhang(张诗按)
Chin. Phys. B . 2017, 26(11): 114206. **doi:** 10.1088/1674-1056/26/11/114206

Optical power limiting of ultrashort hyper-Gaussian pulses in cascade three-level system*

Ji-Cai Liu(刘纪彩)†, Fen-Fen Guo(郭芬芬), Ya-Nan Zhao(赵亚男), and Xing-Zhe Li(李兴哲)

Department of Mathematics and Physics, North China Electric Power University, Beijing 102206, *China*

(Received 31 May 2018; revised manuscript received 3 July 2018; published online 27 September 2018)

Propagation of strong femtosecond hyper-Gaussian pulses in a cascade three-level molecular system is studied by solving numerically the Maxwell–Bloch equations by the iterative predictor-corrector finite-difference time-domain method. Optical power limiting behavior induced by strong nonlinear two-photon absorption is observed for different orders of the femtosecond hyper-Gaussian pulses. Pulses of a higher order temporal profile are found to have a wider power range of optical limiting but a larger output saturation intensity. Both the output saturation value and the damage threshold of optical power limiting decrease with pulse duration increasing. The decrease of the pulse area along the pulse propagation is much slower than that obtained from the two-photon area theorem due to invalidity of the slowly varying amplitude approximation and the monochromatic field hypothesis.

Keywords: optical power limiting, two-photon absorption, ultrashort hyper-Gaussian pulse, cascade three-level system

PACS: 42.65.Re, 42.65.Sf, 32.80.Wr, 42.65.–k **DOI:** 10.1088/1674-1056/27/10/104209

1. Introduction

When nonlinear optical media are exposed to intense laser fields, strong nonlinear optical phenomena occur, such as strong field multi-photon absorption,[1,2] high-order harmonic generation,[3–5] supercontinuum generation,[6,7] optical power limiting,[8–15] self-induced transparency,[16–18] complete population inversion,[19–21] and even creation of particles.[22] It is well known that laser pulse can be characterized by its polarization, field amplitude, carrier temporal profile, pulse duration, carrier frequency, and carrier-envelope phase. Nonlinear optical processes can be coherently controlled by optimizing these parameters.[23–30] For example, shaped pulses have been used to enhance the transient population of excited states and to obtain maximum population inversion;[23–26] the anti-Stokes and Stokes generations can be tailored into a variety of forms in Raman-resonant four-wave-mixing process by manipulating the phase relationship among relevant electromagnetic fields;[27,28] the propagation dynamics of a femtosecond chirped Gaussian pulse and the population distribution in a dense three-level Λ-type atomic medium can be manipulated by changing the sign and size of the chirp coefficient;[29] the robust population inversion against pulse area variation in a V-shaped three-level system can be created by resonant excitation with cross-polarized laser pulse pairs.[30]

The effect of temporal pulse shape on the strong field quantum dynamics involving ultrashort few-cycle pulses has always been one of the focuses of attention of scientists.[31–33] The attosecond electron dynamics and the ultrafast population transfer processes in few-state atomic and molecular systems can be coherently manipulated according to the requirements by using the ultrashort pulses of different field envelopes.[34–36] Conover[37] investigated the effects of pulse shape on strongly driven two-level system and demonstrated experimentally that relatively small changes in the pulse shape of nonresonant radiation can have a dramatic effect on the intensity dependence of the transition probability in a two-level system. Novitsky[38] studied the propagation of subcycle pulses in a two-level medium and found the clear breakdown of the McCall–Hahn area theorem[16,17] for the subcycle pulses of large enough areas, which depends also strongly on the pulse shape. Kumar *et al.*[39] studied optical dipole force and coherence creation on a beam of neutral three-level Λ-like atomic system induced by femtosecond super-Gaussian pulses, and showed that with pulses of high order profiles one can achieve better control of the population transfer process over a large part of the cross sectional plane of the pulse.

In this article, strong nonlinear optical interaction between different orders of femtosecond hyper-Gaussian pulses and a cascade three-level molecular medium is studied. The propagation dynamic behaviors of the ultrashort hyper-Gaussian pulses are investigated by solving the full-wave Maxwell–Bloch equations with the finite-difference time-domain and predictor–corrector numerical method. By tuning the carrier-wave frequency of the field in two-photon resonance with transition between the ground and the uppermost state, optical power limiting behaviors depending on the temporal shape of the pulses are observed for the strong

*Project supported by the National Natural Science Foundation of China (Grant No. 11574082) and the Fundamental Research Funds for the Central Universities, China (Grant No. 2018MS050).

†Corresponding author. E-mail: jicailiu@ncepu.edu.cn

© 2018 Chinese Physical Society and IOP Publishing Ltd

field hyper-Gaussian pulses. Due to the breakdown of the slowly varying amplitude approximation and the invalidity of the monochromatic field condition, the two-photon area theorem[9,10,40,41] is found to be not accurate anymore. The full-wave Maxwell's and optical Bloch equations that describe the interaction of a three-level system with strong laser fields are presented in Subsection 2.1. The definition of two-photon area and the two-photon area theorem are given in Subsection 2.2. The results of numerical simulations by solving the full-wave Maxwell–Bloch equations are discussed in Section 3, and our findings are summarized in Section 4.

2. Theoretical methods

2.1. Maxwell–Bloch equations for three-level system

The propagation of strong femtosecond laser fields in a three-level molecular medium is studied here. Based on the semiclassical theory, Maxwell's equations and density matrix equations are used respectively to describe the laser fields and the quantum system. Taking into account the phenomenological relaxation effect, the density matrix equation derived from the Schrodinger equation can be written as[42]

$$\frac{\partial \rho_{ij}}{\partial t} = -\frac{\mathrm{i}}{\hbar}\left[H,\rho\right]_{ij} - \gamma_{ij}\left(\rho_{ij}-\rho_{ij}^{0}\right). \tag{1}$$

Here H is the Hamiltonian of the quantum system, and γ_{ij} is the relaxation rate of the density matrix element ρ_{ij}. The three energy levels of the molecular system are marked as 1, 2, and 3. By the use of the substitutions $\rho_{12}=(\mu_1+\mathrm{i}v_1)/2$, $\rho_{23}=(\mu_2+\mathrm{i}v_2)/2$, and $\rho_{13}=(\mu_3+\mathrm{i}v_3)/2$, the Bloch equations for a three-level system are derived from the density matrix equation (1) containing relaxation effects as follows:

$$\begin{aligned}
\frac{\partial \mu_1}{\partial t} &= -\omega_{21}v_1 + \frac{\boldsymbol{E}\cdot(\boldsymbol{d}_{22}-\boldsymbol{d}_{11})v_1}{\hbar} + \frac{\boldsymbol{E}\cdot(\boldsymbol{d}_{23}v_3+\boldsymbol{d}_{13}v_2)}{\hbar} \\
&\quad -\gamma_{12}\mu_1, \\
\frac{\partial v_1}{\partial t} &= \omega_{21}\mu_1 - \frac{\boldsymbol{E}\cdot(\boldsymbol{d}_{22}-\boldsymbol{d}_{11})\mu_1}{\hbar} - \frac{\boldsymbol{E}\cdot(\boldsymbol{d}_{23}\mu_3-\boldsymbol{d}_{13}\mu_2)}{\hbar} \\
&\quad -\frac{2}{\hbar}\boldsymbol{E}\cdot\boldsymbol{d}_{12}(\rho_{11}-\rho_{22}) - \gamma_{12}v_1, \\
\frac{\partial \mu_2}{\partial t} &= -\omega_{32}v_2 + \frac{\boldsymbol{E}\cdot(\boldsymbol{d}_{33}-\boldsymbol{d}_{22})v_2}{\hbar} - \frac{\boldsymbol{E}\cdot(\boldsymbol{d}_{13}v_1+\boldsymbol{d}_{12}v_3)}{\hbar} \\
&\quad -\gamma_{23}\mu_2, \\
\frac{\partial v_2}{\partial t} &= \omega_{32}\mu_2 - \frac{\boldsymbol{E}\cdot(\boldsymbol{d}_{33}-\boldsymbol{d}_{22})\mu_2}{\hbar} - \frac{\boldsymbol{E}\cdot(\boldsymbol{d}_{13}\mu_1-\boldsymbol{d}_{12}\mu_3)}{\hbar} \\
&\quad -\frac{2}{\hbar}\boldsymbol{E}\cdot\boldsymbol{d}_{23}(\rho_{22}-\rho_{33}) - \gamma_{23}v_2, \\
\frac{\partial \mu_3}{\partial t} &= -\omega_{31}v_3 + \frac{\boldsymbol{E}\cdot(\boldsymbol{d}_{33}-\boldsymbol{d}_{11})v_3}{\hbar} + \frac{\boldsymbol{E}\cdot(\boldsymbol{d}_{23}v_1-\boldsymbol{d}_{12}v_2)}{\hbar} \\
&\quad -\gamma_{13}\mu_3, \\
\frac{\partial v_3}{\partial t} &= \omega_{31}\mu_3 - \frac{\boldsymbol{E}\cdot(\boldsymbol{d}_{33}-\boldsymbol{d}_{11})\mu_3}{\hbar} - \frac{\boldsymbol{E}\cdot(\boldsymbol{d}_{23}\mu_1-\boldsymbol{d}_{12}\mu_2)}{\hbar} \\
&\quad -\frac{2}{\hbar}\boldsymbol{E}\cdot\boldsymbol{d}_{13}(\rho_{11}-\rho_{33}) - \gamma_{13}v_3,
\end{aligned}$$

$$\begin{aligned}
\frac{\partial \rho_{11}}{\partial t} &= \frac{\boldsymbol{E}}{\hbar}\cdot(\boldsymbol{d}_{12}v_1+\boldsymbol{d}_{13}v_3) + \gamma_{22}\rho_{22}, \\
\frac{\partial \rho_{22}}{\partial t} &= -\frac{\boldsymbol{E}}{\hbar}\cdot(\boldsymbol{d}_{12}v_1-\boldsymbol{d}_{23}v_2) - \gamma_{22}\rho_{22} + \gamma_{33}\rho_{33}, \\
\frac{\partial \rho_{33}}{\partial t} &= -\frac{\boldsymbol{E}}{\hbar}\cdot(\boldsymbol{d}_{13}v_3+\boldsymbol{d}_{23}v_2) - \gamma_{33}\rho_{33},
\end{aligned} \tag{2}$$

where μ_i and v_i are real-valued quantities related to the coherence ρ_{ij} ($i\neq j$, and $i,j=1,2,3$), ρ_{ii} is the population occupation of the state i, $\hbar\omega_{ij}$ is the excitation energy from state j to state i, and $\boldsymbol{d}_{ij}=\boldsymbol{d}_{ji}$ are the permanent electric dipole moments or the transition electric dipole moments of the molecule. For a cascade three-level system with central inversion symmetry, $d_{ii}=d_{13}=0$.

The external field is written as $\boldsymbol{E}(t,\boldsymbol{r})=\boldsymbol{e}F(t)\cos(\omega t-\boldsymbol{k}\cdot\boldsymbol{r})$, with polarization vector $\boldsymbol{e}$, temporal envelope $F(t)$, carrier-wave frequency ω, and wave vector $\boldsymbol{k}$. Assuming that the incident electromagnetic field with polarization parallel to the x axis propagates along the z axis $E_x(t,z)$, the Maxwell's equations describing the evolution of the field during propagation can be written as[43]

$$\begin{aligned}
\frac{\partial H_y}{\partial t} &= -\frac{1}{\mu_0}\frac{\partial E_x}{\partial z}, \\
\frac{\partial E_x}{\partial t} &= -\frac{1}{\varepsilon_0}\frac{\partial H_y}{\partial z} - \frac{1}{\varepsilon_0}\frac{\partial P_x}{\partial t},
\end{aligned} \tag{3}$$

where μ_0 and ε_0 are, respectively, the permeability and permittivity of free space, P_x is the macroscopic nonlinear polarization determined by the ensemble average of the expectation value of the dipole moment operator, and expressed as

$$P_x = N\langle d_x\rangle = N\,\mathrm{tr}\left(d_x\rho\right), \tag{4}$$

where N is the molecular number density of the medium.

2.2. Two-photon area theorem

With slowly varying amplitude and phase approximation, the propagation of the laser field in a cascade three-level system under the two-photon resonant condition can be described by the two-photon area theorem as[9,10]

$$\frac{\mathrm{d}}{\mathrm{d}z}\theta(z) = -\frac{2}{L}\sin^2\frac{\theta(z)}{2}, \tag{5}$$

and the two-photon area of the pulse $\theta(z)$ is proportional to the energy fluence of the field and given as

$$\theta(z) = \zeta\int_{-\infty}^{+\infty} I(z,t)\,\mathrm{d}t. \tag{6}$$

Here $I(z,t)$ is the light intensity, L is the length of two-photon absorption, and ζ is the two-photon absorption coefficient, and they are given, respectively, as

$$\begin{aligned}
L &= \frac{c\varepsilon_0\hbar\sqrt{1+\kappa^2}}{4N\omega\zeta_{13}}, \\
\zeta &= \frac{4\zeta_{13}\sqrt{1+\kappa^2}}{c\varepsilon_0\hbar},
\end{aligned}$$

$$\zeta_{13} = \frac{d_{12}d_{23}}{4(\omega - \omega_{21})}. \tag{7}$$

The parameter κ depends on the dynamical Stark shifts Δ_i ($i = 1, 3$) and the coupling parameter Δ_{13},

$$\kappa = \frac{\Delta_3 - \Delta_1}{2\Delta_{13}},$$
$$\Delta_i = \frac{G_{2i}^2 \omega_{2i}}{2(\omega^2 - \omega_{2i}^2)},$$
$$\Delta_{13} = \frac{G_{12}G_{23}}{4(\omega - \omega_{21})}. \tag{8}$$

Here $G_{ij} = d_{ij}E(t,z)/\hbar$ is the Rabi frequency. According to the two-photon area theorem, the evolution of the two-photon area of the pulse follows a piecewise function that depends on the initial value of the pulse area θ_0. With the initial pulse area $2(m-1)\pi < \theta_0 < 2m\pi$, where m is a natural number, the area of the pulse during propagation will be confined in the region $2(m-1)\pi < \theta(z) < \theta_0$. Pulses with input areas slightly below $2m\pi$ will propagate without significantly changing the area up to a long distance characterized by $z_c = -L\cot(\theta_0/2)$, and then will be rapidly reduced to an area close to $2(m-1)\pi$.[9]

3. Results and discussion

The strong field nonlinear optical interaction between ultrashort hyper-Gaussian pulses and a cascade three-level system is studied by solving the Maxwell–Bloch equations (2)–(3) with an iterative predictor-corrector finite-difference time-domain numerical scheme. The temporal shape of the hyper-Gaussian laser field is written as $F(t) = F_0 \exp(-\ln 2/2(t-t_0)^{2n}/(\tau/2)^{2n})$, where F_0 is the peak value of the field amplitude, τ is the full-width at half-maximum (FWHM) of the temporal profile of the light intensity $I(t) = c\varepsilon_0 F^2(t)/2$, and n is the order of the hyper-Gaussian pulse which determines the temporal shape of the pulse. The pulse has a Gaussian shape with $n = 1$ and the pulse shape tends to be rectangular with the increase of n. The carrier-wave frequency of the laser pulse is tuned in two-photon resonance with the two-photon absorption state, i.e. $\omega = \omega_{31}/2$. The energy levels and the dipole moments for the three-level system are taken from 4,4'-bis(dimethylamino) stilbene molecule[11,44] with $\omega_{21} = 3.46$ eV, $\omega_{31} = 4.27$ eV, $d_{21} = 10.433$ deb (1 deb = 3.33564×10^{-3} C·m), $d_{32} = 18.497$ deb, and $d_{ii} = 0$. The molecules are in the ground state before the incidence of the laser pulse, namely $\rho_{11}^{(0)} = 1$, $\rho_{22}^{(0)} = \rho_{33}^{(0)} = 0$. The relaxation rates $\gamma_{22} = 10^9$/s and $\gamma_{33} = 10^{12}$/s, and the rate of decoherence $\gamma_{ij} = 10^{12}$/s. The molecular number density $N = 7.0\times10^{19}$/cm^3.

The propagation dynamic behaviors of the hyper-Gaussian pulses of different temporal profile orders are numerically simulated by solving the Maxwell–Bloch equations (2) and (3). Figure 1 shows the evolution of the output field intensity at the propagation distance $z = 7.0$ μm as a function of the input field intensity for three different orders of the hyper-Gaussian pulses ($n = 1$, 2, 3) with an equal initial FWHM $\tau = 5$ fs. One can see obviously the two-photon absorption induced optical power limiting behaviors for all the three orders of the hyper-Gaussian pulses. By comparing the three lines shown in Fig. 1, one can also see that with the increase of the input field intensity, the optical limiting behavior breaks down earlier for the lower order pulse. On the other hand, the lower order pulse has a smaller output intensity of optical limiting. For $n = 1$, the optical limiting effect breaks down with a saturation output intensity $I_s^{(1)} = 3.8\times10^{11}$ W/cm^2 when the input field intensity increases to 3.0×10^{12} W/cm^2. For $n = 2$, the optical limiting effect breaks down with a saturation output intensity $I_s^{(2)} = 5.6\times10^{11}$ W/cm^2 when the input field intensity increases to 3.12×10^{12} W/cm^2. For $n = 3$, the optical limiting effect breaks down with a saturation output intensity $I_s^{(3)} = 6.5\times10^{11}$ W/cm^2 when the input field intensity increases to 3.3×10^{12} W/cm^2. The output intensities of optical limiting increase with the increase of n, but their differences decrease with the increase of n, and become invisible for high order pulses. That is because the rate of change of the pulse shape with respect to the pulse order n slows down with the increase of n.

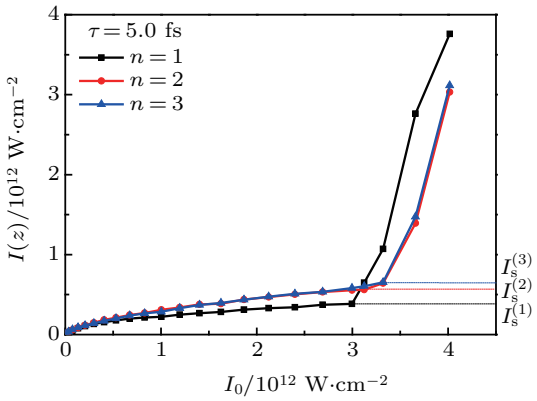


Fig. 1. (color online) Optical power limiting behaviors of strong hyper-Gaussian laser pulses with FWHM $\tau = 5.0$ fs for three values of order n of incident hyper-Gaussian pulses: 1 (rectangle), 2 (circle), and 3 (triangle).

The optical power limiting behaviors of strong hyper-Gaussian laser pulses with FWHM $\tau = 7.5$ fs and 10 fs are presented in Figs. 2 and Fig. 3, respectively. They have very similar behaviors. Both cases show that with the increase of the input field intensity, the optical limiting effect breaks down first for pulses of a small value of n, but with a small output intensity. The difference of output intensity of optical limiting between $I_s^{(2)}$ and $I_s^{(3)}$ is smaller than the difference between $I_s^{(2)}$ and $I_s^{(3)}$. By comparing Figs. 1, 2, and 3, one can see that both the output saturation values and the damage thresholds of

optical power limiting are smaller for pulses of a longer duration.

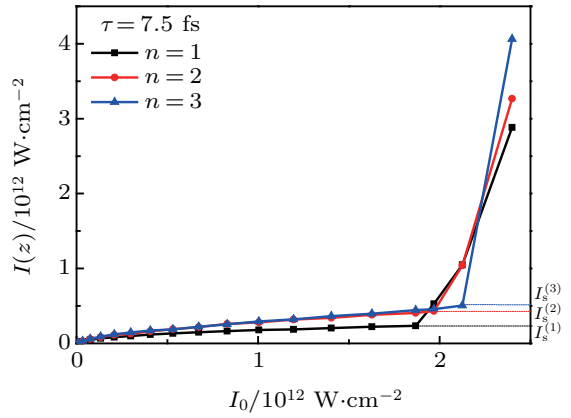


Fig. 2. (color online) Optical power limiting behaviors of strong hyper-Gaussian laser pulses with FWHM $\tau = 7.5$ fs for three values of order n of the incident hyper-Gaussian pulses: 1 (rectangle), 2 (circle), and 3 (triangle).

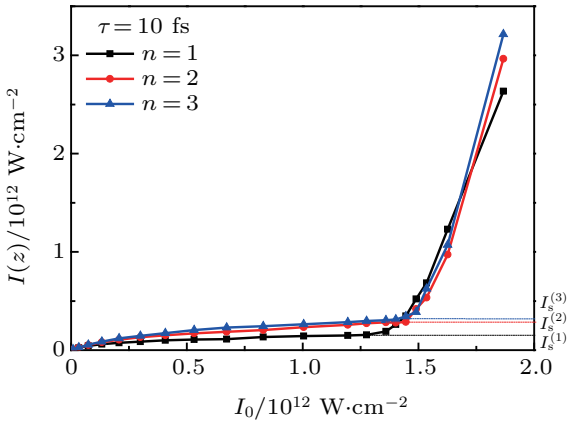


Fig. 3. (color online) Optical power limiting behaviors of strong hyper-Gaussian laser pulses with FWHM $\tau = 10$ fs for three different values of order n of the incident hyper-Gaussian pulses: 1 (rectangle), 2 (circle), and 3 (triangle).

The above results show that the two-photon absorption induced optical power limiting behaviors of the ultrashort hyper-Gaussian pulses are consistent qualitatively with the two-photon area theorem (Eq. (5)). For example, the optical power limiting effect breaks down with initial two-photon areas around 1.5π. Since the two-photon area of a pulse is proportional to its pulse width τ and field intensity $I(z,t)$ according to Eq. (6), the output saturation intensity $I_s^{(n)}$ and the damage threshold intensity are smaller for pulses of a bigger τ. And for pulses of the same peak intensity I_0 and pulse duration τ, the pulse with a large n has a small input two-photon area θ_0, therefore, the intensity range of optical power limiting is broad for the pulse of a high order. However, due to invalidity of the slowly varying amplitude approximation and monochromatic field hypothesis, the two-photon area theorem is not accurate for the quantitative description of the evolution of ultrashort hyper-Gaussian pulses. For example, after the breakdown of the optical power limiting effect, the speed rate of field intensity growth is much slower for the ultrashort pulses than that given by the two-photon area theorem due to the generation of new field components during pulse propagation.

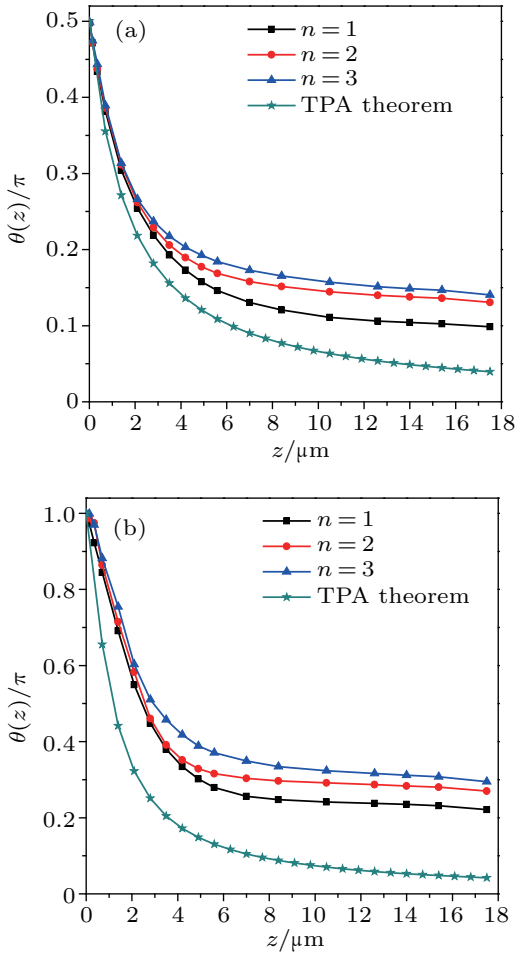


Fig. 4. (color online) Evolutions of the two-photon areas of the hyper-Gaussian pulses with$\tau = 5.0$ fs. (a) $\theta_0 = 0.5\pi$, peak field intensities for $n = 1$ (rectangle), 2 (circle), and 3 (triangle) are respectively $I_0 = 0.808 \times 10^{12}$ W/cm^2, 0.866×10^{12} W/cm^2, and 0.872×10^{12} W/cm^2. (b) $\theta_0 = \pi$, peak field intensities for $n = 1$ (rectangle), 2 (circle), and 3 (triangle) are respectively $I_0 = 1.616 \times 10^{12}$ W/cm^2, 1.731×10^{12} W/cm^2, and 1.744×10^{12} W/cm^2. Results given by two-photon area theorem (Eq. (5)) are shown with star-dotted lines.

The evolutions of the two-photon area $\theta(z)$ (Eq. (6)) along the pulse propagation for different orders of the 5.0 fs incident hyper-Gaussian pulses are shown in Fig. 4. The initial two-photon areas are respectively 0.5π (Fig. 4 (a)) and π (Fig. 4 (b)). At the early stage of pulse propagation, the areas of the pulses drop drastically due to strong two-photon absorption, and after a short propagation distance of about $z_c \sim 4.0$ μm the pulse areas then change slowly. For different orders of pulses, the areas have similar dependence on the propagation distance z during the fast decrease stage, but the differences become visible around and after the characteristic distance z_c. It is worth noting that although the results given by the two-photon area theorem Eq. (5) show the same trend of evolution, the rates of change of the pulse areas for the ultrashort hyper-Gaussian pulses as a function of propagation distance z are slower than that given by the two-photon area the-

orem, and the theorem gives much smaller area after the characteristic distance z_c. For example, the areas are about 0.04 for both initial areas of 0.5π and 1.0π at $z = 17.5$ μm by the area theorem. But the ultrashort hyper-Gaussian pulses give very different values, respectively 0.1π and 0.22π at $z = 17.5$ μm for initial areas of 0.5π and 1.0π with $n = 1$, and these values increase with the increase of pulse order n. That is because the two-photon area theorem is derived for single-color field, and it neglects the relaxation dynamic behavior by the use of amplitude equations. But for the ultrashort laser pulses, we solve directly the full-wave Maxwell–Bloch equations (2)–(3) and take into account the phenomenological relaxation effect. Due to the strong nonlinear optical effects, new field components such as hyper-Ramans, odd harmonics and resonant fields starting from spontaneous emissions are generated during pulse propagation, and the consideration of these new fields neutralizes the two-photon area theorem and slows down the decrease of the pulse area. And for the pulses of a large n, the new fields are generated earlier than those of a small n, therefore there are stronger deviations from the two-photon area theorem.

4. Conclusions

We have studied here the optical power limiting behaviors of strong femtosecond hyper-Gaussian pulses induced by two-photon absorption in a cascade three-level system. It is found that the optical power limiting behavior breaks down earlier for pulses of a lower order, but with a smaller output intensity of optical limiting. Since the rate of change of the pulse shape with respect to the pulse order n slows down with the increase of n, the difference between the output saturation intensities of optical limiting also decreases with the increase of n, and becomes invisible for high order pulses. With the decrease of the pulse duration, both the output saturation intensity and the power range of optical limiting increase. Although the two-photon absorption induced optical power limiting behaviors of the ultrashort hyper-Gaussian pulses can be described qualitatively with the two-photon area theorem, due to the generation of the new fields during propagation of the hyper-Gaussian pulse, the two-photon area theorem is not strict anymore, and the decrease of the pulse area along the propagation is much slower than that obtained from the two-photon area theorem.

References

[1] Corkum P B 1993 *Phys. Rev. Lett.* **71** 1994
[2] Trallero-Herrero C, Cardoza D, Weinacht T C and Cohen J L 2005 *Phys. Rev. A* **71** 013423
[3] Teubner U and Gibbon P 2009 *Rev. Mod. Phys.* **81** 445
[4] Mahieu B, Stremoukhov S, Gauthier D, Spezzani C, Alves C, Vodungbo B, Zeitoun P, Malka V, De Ninno G and Lambert G 2018 *Phys. Rev. A* **97** 043857
[5] Liu J C, Kohler M C, Keitel C H and Hatsagortsyan K Z 2011 *Phys. Rev. A* **84** 063817
[6] Corkum P B, Roll, C and Srinivasan-Rao T 1986 *Phys. Rev. Lett.* **57** 2268
[7] Dudley J M, Genty G and Coen S 2006 *Rev. Mod. Phys.* **78** 1135
[8] Tutt L W and Boggess T F 1993 *Prog. Quantum Electron.* **17** 299
[9] Liu J C, Wang C K and Gel'mukhanov F 2007 *Phys. Rev. A* **76** 053804
[10] Liu J C, Wang C K and Gel'mukhanov F 2007 *Phys. Rev. A* **76** 043422
[11] Wang C K, Liu J C, Zhao K, Sun Y P and Luo Y 2007 *J. Opt. Soc. Am. B* **24** 2436
[12] Hermann J A 1984 *J. Opt. Soc. Am. B* **1** 729
[13] Zhang Y J, Li X Z, Liu J C and Wang C K 2016 *Chin. Phys. B* **25** 013302
[14] Miao Q, Zhao P, Sun Y P and Wang C K 2009 *Acta Phys. Sin.* **58** 5455 (in Chinese)
[15] Fang L B, Zhong S H and Shen W Z 2017 *Chin. Phys. Lett.* **34** 098101
[16] McCall S L and Hahn E L 1967 *Phys. Rev. Lett.* **18** 908
[17] Allen L and Eberly J H 1987 *Optical Resonance and Two-Level Atoms* (New York: Dover Publications Inc.) p. 90
[18] Liu J C, Zhang Y Q and Chen L 2014 *J. Mod. Opt.* **61** 781
[19] Kaluža M and Muckerman J T 1995 *Phys. Rev. A* **51** 1694
[20] Cao J, Bardeen C J and Wilson K R 1998 *Phys. Rev. Lett.* **80** 1406
[21] Vala J and Kosloff R 2001 *Opt. Express* **8** 238
[22] Di Piazza A, Müller C, Hatsagortsyan K Z and Keitel C H 2012 *Rev. Mod. Phys.* **84** 1177
[23] Liu J C, Felicissimo V C, Guimaraes F F, Wang C K and Gel'mukhanov F 2008 *J. Phys. B: At. Mol. Opt. Phys.* **41** 074016
[24] Jha P K, Eleuch H and Rostovtsev Y V 2010 *Phys. Rev. A* **82** 045805
[25] Dudovich N, Oron D and Silberberg Y 2002 *Phys. Rev. Lett.* **88** 123004
[26] Zhang Z, Yang X and Yan X 2013 *J. Opt. Soc. Am. B* **30** 1017
[27] Ohae C, Zheng J, Ito K, Suzuki M, Minoshima K and Katsuragawa M 2018 *Opt. Express* **26** 1452
[28] Zheng J and Katsuragawa M 2015 *Sci. Rep.* **5** 8874
[29] Wang Z D, Liang B, Liu Z B and Fan X J 2010 *Acta Phys. Sin.* **59** 7041 (in Chinese)
[30] Mantei D, Förstner J, Gordon S, Leier Y A, Rai A K, Reuter D, Wieck A D and Zrenner A 2015 *Sci. Rep.* **5** 10313
[31] Winterfeldt C, Spielmann C and Gerber G 2008 *Rev. Mod. Phys.* **80** 117
[32] Vitanov N V, Rangelov A A, Shore B W and Bergmann K 2017 *Rev. Mod. Phys.* **89** 015006
[33] Pazourek R, Nagele S and Burgdörfer J 2015 *Rev. Mod. Phys.* **87** 765
[34] Goulielmakis E, Yakovlev V S, Cavalieri A L, Uiberacker M, Pervak V, Apolonski A, Kienberger R, Kleineberg U and Krausz F 2007 *Science* **317** 769
[35] Wefers M M and Nelson K A 1993 *Science* **262** 1381
[36] Liu J C 2014 *J. Electron. Spectrosc. Relat. Phenom.* **195** 132
[37] Conover C W S 2011 *Phys. Rev. A* **84** 063416
[38] Novitsky D V 2012 *Phys. Rev. A* **86** 063835
[39] Kumar P, Kumar P and Sarma A K 2014 *Phys. Rev. A* **89** 033422
[40] Belenov E M and Poluektov I A 1969 *Sov. Phys.-JETP* **29** 754
[41] Tan-no N, Yokoto K and Inaba H 1972 *Phys. Rev. Lett.* **29** 1211
[42] Boyd R W 2010 *Nonlinear Optics*, 3rd edn. (Singapore: Elseiver Pte Ltd.) p. 155
[43] Jackson J D 1998 *Classical Electrodynamics*, 3rd edn. (New York: John Wiley & Sons, Inc.) p. 2
[44] Liu J C, Zhao K, Song Y Z and Wang C K 2006 *Acta Phys. Sin.* **55** 1803 (in Chinese)